# Engineering Proceedings

Switzerland | Universities and research institutions | Media Ranking

Country

Switzerland

SCIMAGO INSTITUTIONS RANKINGS

SCImago Media Rankings

Subject Area and Category

Engineering
- Biomedical Engineering
- Electrical and Electronic Engineering
- Industrial and Manufacturing Engineering
- Mechanical Engineering

Publisher

Multidisciplinary Digital Publishing Institute (MDPI)

SJR 2025

0.254 Q3

H-Index

25

Publication type

Journals

ISSN

26734591

Coverage

2020-2025

Information

Home ↗

How to publish in this journal ↗

engproc@mdpi.com ↗

Scope

Engineering Proceedings (ISSN 2673-4591) provides an advanced forum for studies on engineering that are presented at an academic conference. It publishes proceeding papers and conference reports on particular subjects. The aim of Engineering Proceedings is to help the conference organizers to publish cutting-edge, original, and peer-reviewed outputs resulting from the conference. All kinds of materials that result from the conference, including but not limited to presentations, posters, and videos, can be published along with their paper in the journal if accepted by the academic editor after peer review. Scope: -Chemical engineering- Civil engineering- Electric and electronic engineering- Mechanical engineering- Materials engineering- Bioengineering- Environmental engineering- Computer and software engineering- Biomedical engineering

## Quartiles

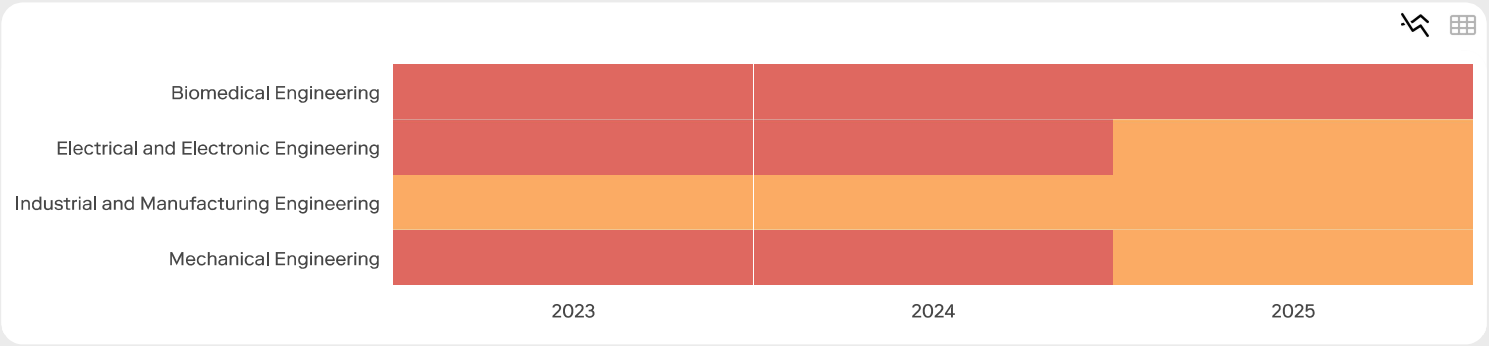


## Find similar journals

All quartiles | All countries | All subject categories | Clear filters | Download

Only Open Access Journals

1 - Technologies

65%

similarity

2 - Applied Sciences (Switzerland)

63%

similarity

3 - Applied System Innovation

60%

similarity

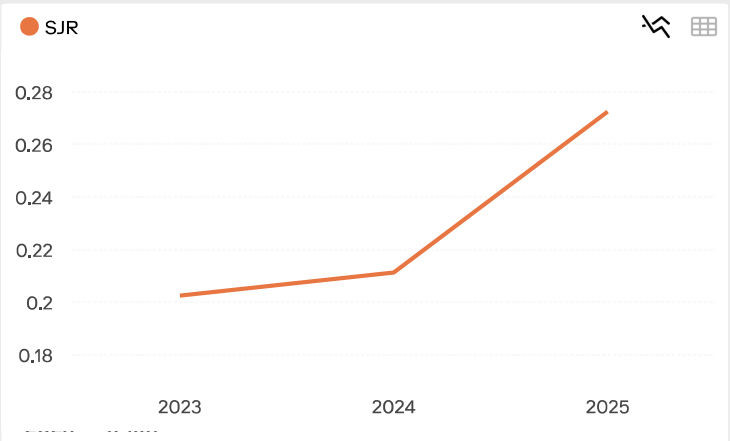


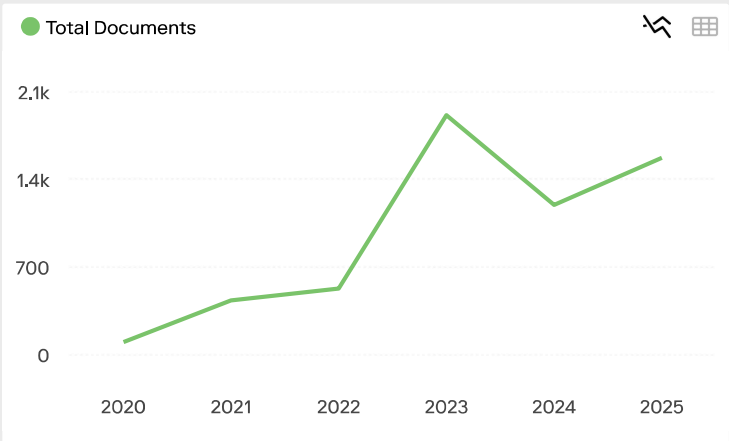

External Cites per Doc
Cites per Doc

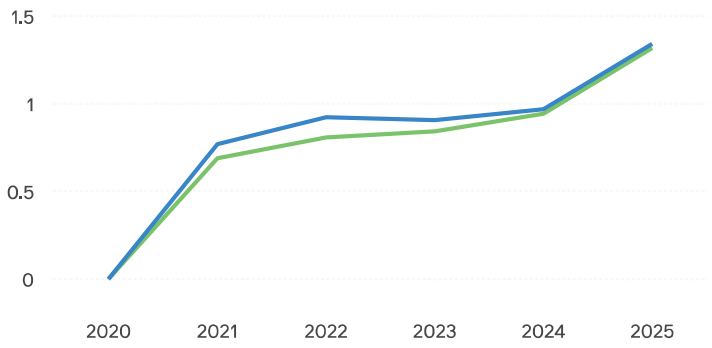


% International Collaboration

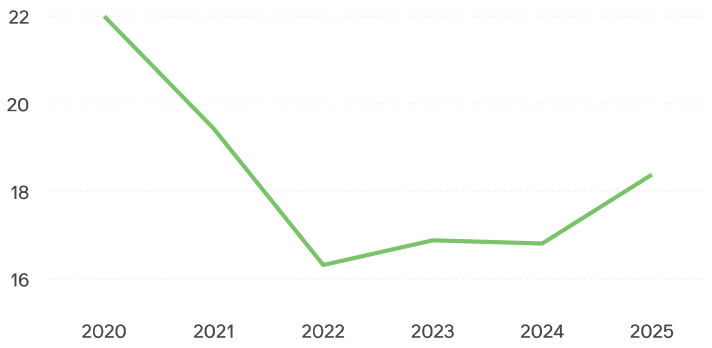


Cited documents
Uncited documents

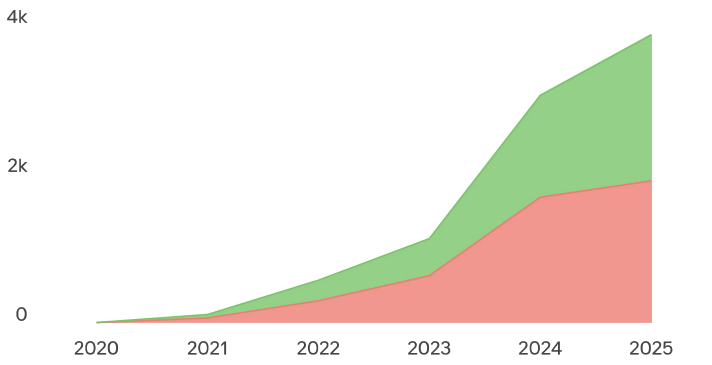


% Female Authors

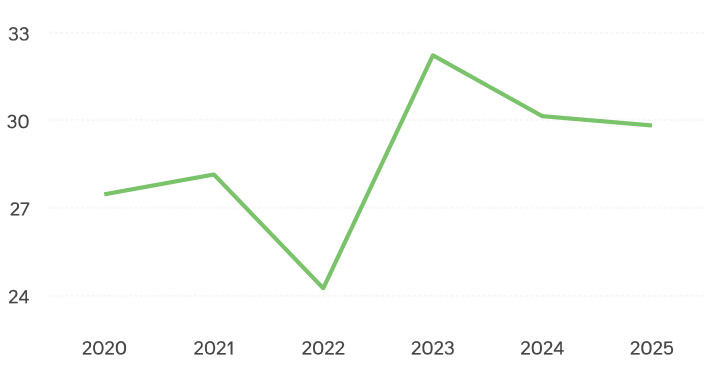


Estimated APC

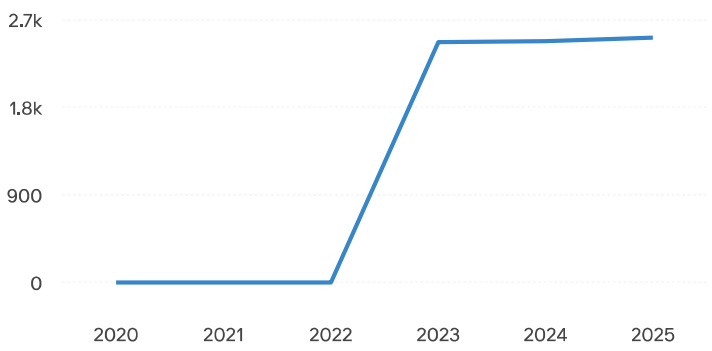


Estimated financial value

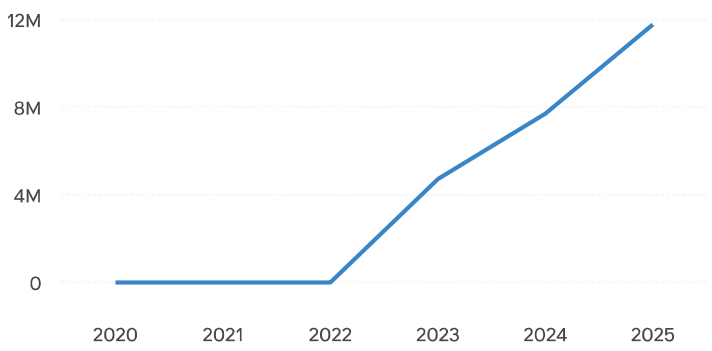


Total Cites
Self-Cites

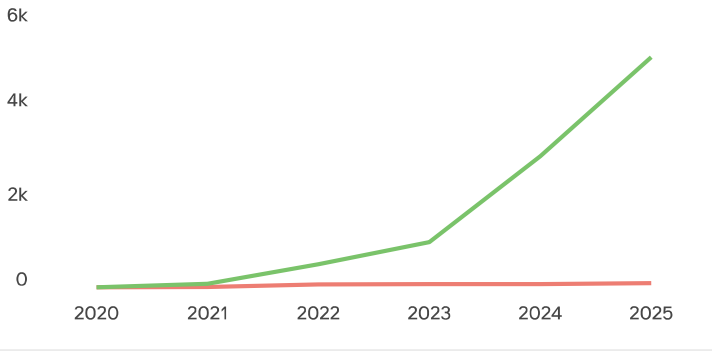


Citations per document

Citable documents
Non-citable documents

engineering proceedings

MDPI

*Proceeding Paper*

# Visible-Light-Induced Photocatalytic Degradation of Fast Green FCF and Orange II Dye by $Yb_2O_3$ Nanoparticles †

**Nashra Fatima [1], Ekhlakh Veg [1,2] and Tahmeena Khan [1,*]**

[1] Department of Chemistry, Integral University, Lucknow 226026, India; ffnashra@student.iul.ac.in (N.F.); akhlakhbeg123@gmail.com or akhlakh@student.iul.ac.in (E.V.)
[2] Department of Chemistry, Isabella Thoburn College, Lucknow 226020, India
* Correspondence: tahminakhan30@yahoo.com or tahmeenak@iul.ac.in; Tel.: +91-9793232443
† Presented at the 6th International Electronic Conference on Applied Sciences, 9–11 December 2025; Available online: https://sciforum.net/event/ASEC2025.

**Abstract**

The quest for efficient photocatalytic materials for eliminating synthetic dyes like Orange II Sodium Salt and Fast Green FCF (For Coloring Food) has been spurred by the mounting environmental problems associated with these dyes. Due to their excellent electrical characteristics, thermal stability, and potential to reduce electron–hole recombination, ytterbium oxide ($Yb_2O_3$) and other rare-earth metal oxides are gaining popularity. This study synthesized $Yb_2O_3$ nanoparticles and assessed their photocatalytic activity when exposed to visible light. Significant degradation efficiencies were revealed by the spectrophotometric analysis, suggesting that $Yb_2O_3$ is an effective nanocatalyst for dye remediation applications. The results demonstrate how rare-earth-based nanomaterials can improve environmentally friendly and sustainable wastewater treatment methods, supporting ongoing environmental cleanup initiatives.

**Keywords:** Fast Green FCF; Orange II Sodium Salt; photocatalysis; $Yb_2O_3$; water management; pollution remediation; pollutant removal

## 1. Introduction

Water is an essential commodity for ecosystems and people equally. One of the most severe problems facing humanity worldwide now is the contamination of water [1]. Pollutants from industrial, agricultural, and human activities include pesticides, fertilizers, dyes, heavy metals, and surface-active compounds [2]. Dyes are commonly used as coloring agents in a range of industries to improve the appearance and value of products. Each year, more than 10,000 dyes totalling more than $7 \times 10^5$ metric tons are produced, primarily for printing and dyeing [3]. Due to their capacity to impart vivid and long-lasting colors, dyes are a significant class of environmental pollutants that are widely utilized in sectors like textiles, paper, plastics, leather, and cosmetics [4]. There are dyes that are both natural and manufactured. Natural dyes are colorants or dyes derived from invertebrates, plants, or minerals. Most natural dyes are vegetable colors procured from plants, their different parts, and other biological sources like fungi. Chemical compounds that are deliberately created in laboratories, mostly from coal tar or petroleum-based chemicals, are known as synthetic dyes. Natural dyes are not as frequently utilized as synthetic dyes despite their historical relevance and beneficial effects on the environment because of their limited color range, unpredictable outcomes, high production costs, and poor fading resistance [5].



Published: 5 March 2026

The chemical structure and application of dyes define them. The pigment's color is derived from a class of molecules known as chromophores. Numerous functional groups, including azo, anthraquinone, methine, nitro, aryl methane, carbonyl, etc., form the basis for these chromophore-containing dyes. Electrons that are transferred from or provided to substituent groups to create or enhance the color of the chromophore are known as auxochromes. Amines, carboxyls, sulfonic acids, and hydroxyls are the four most common auxochromes [6]. For procedures including dying, mending, softening, and washing, the textile industry utilizes a lot of water. It has been found that 15% of the pigment is washed out in water during the dying process and becomes effluent [7]. Due to the chemicals' significant potential to have detrimental impacts on natural water sources, the extensive industrial release of dyes into the environment raises serious ecological concerns [8]. When wastewater from different industries containing excessive concentrations of dyes enters water bodies. Plants and aquatic organisms have less access to light, which has a negative impact, and it makes self-purification impossible [9]. Aquatic plants and wildlife are impacted as a result of a decrease in photosynthesis and oxygen levels. Since algae are at the base of the food chain, light absorption predominantly reduces their photosynthetic activity, which has a significant impact on all organisms above them [10]. Long-term dye exposure can have harmful effects on the aquatic environment, including low aerobic biodegradability, accumulation in sediments, especially in aquatic life forms, and breakdown of pollutants into carcinogenic or mutagenic compounds. Numerous colors and the byproducts of their breakdown are harmful to life, carcinogenic, and mutagenic. Even minute concentrations in the water for days can have a significant negative impact on the transparency and quality of bodies of water like rivers, lakes, and others, harming the aquatic ecosystem. When they are consumed, gut microbes break them down, damaging DNA [11].

Dyes are extremely toxic and perhaps carcinogenic, generating several new health issues in both humans and animals in addition to wreaking havoc on the environment [12]. Textile dye toxicity to humans can be classified as either acute or chronic/genotoxic. Skin irritation and skin sensitization are the primary issues associated with acute poisoning with textile dyes, which can occur by oral intake and inhalation. The main long-term health risk associated with some textile dyes is chronic or genotoxicity. This became evident when, between 1930 and 1960, a significant prevalence of bladder cancer was noted among factory workers engaged in the production of specific dyes. Fuchsine, auramine, benzidine, and two naphthylamines were the specific substances involved [13]. Respiratory issues brought on by breathing in dye particles are the most frequent concern about colorants. A person's immune system may occasionally be impacted by a dye; in severe circumstances, this could cause a violent reaction the next time the person breathes in the color. This condition is referred to as respiratory sensitization and manifests as sneezing, wet eyes, itching, wheezing, and coughing—all of which are symptoms of asthma [14]. The human body can absorb dyes through the gastrointestinal tract, respiratory system, or skin. Ingested dyes often pass through the intestinal epithelium and into the bloodstream after being absorbed by the stomach and small intestine. Particles of airborne dye can enter the bloodstream through the respiratory system after being inhaled and lodging in the lungs. Certain colors have been shown to penetrate the skin and enter the bloodstream, especially when they come into contact with damaged or broken skin. After being absorbed, dyes can circulate throughout the body and build up in different organs and tissues. Adipose tissue and organs such the liver, kidneys, lungs, spleen, and brain have all been found to contain dyes and their metabolites. Adipose tissue also has a tendency to accumulate dyes. Human dye bioaccumulation is a complicated process that is impacted by a number of factors, such as exposure dose, duration, frequency, individual metabolism, and physiological parameters. Over time, the body may gradually accumulate dyes due to prolonged exposure to low

https://doi.org/10.3390/engproc2026124054

quantities from diet or environmental sources. Furthermore, specific metabolic pathways can convert dyes into metabolites with varying toxicity profiles and varying levels of bioavailability. For instance, gut bacteria have the ability to convert certain azo dyes into aromatic amines, which are recognized carcinogens and may increase the carcinogenicity of azo dyes [15]. Among these dyes, Orange II and Fast Green FCF dyes are well known for both their uses and adverse consequences. Fast Green FCF ($C_{37}H_{34}N_2Na_2O_{10}S_3$), a triphenylmethane dye with a molecular weight of 808.84 g/mol, is widely used as a food colorant and in textiles, while Orange II ($C_{16}H_{11}N_2NaO_4S$), an azo dye with a molecular weight of 248.71 g/mol, is utilized in the leather, paper, and cosmetics industries [16]. The environment and people are negatively impacted by both of these colors. Therefore, creating economical and effective ways to break down these dyes is crucial. Dyes have been eliminated from wastewater discharge using a variety of physicochemical techniques. However, many chemical or physical approaches have intrinsic flaws that render them unfeasible from an economic standpoint. The disadvantages include the necessity for labor-intensive operations, substantial sludge generation that could result in secondary contamination, higher energy and chemical requirements, and partial removal of organic metabolites. Enzymes, bacteria, algae, and other microorganisms have also been used to try dye breakdown, although each approach has disadvantages of its own [17]. The photocatalytic technique stands out as a cost-effective, sustainable, and environmentally safe way to remediate dye wastewater. This effective technique makes use of sunshine, which supplies energy higher than the photocatalysts' band gap. As a result, electrons get excited and travel from the valence band to the conduction band, creating electron hole pairs that have the ability to break down wastewater contaminants. It is desirable because of its affordability, sustainability, and capacity to totally break down pollutants when exposed to sunshine. One practical solution to reduce the negative effects of industrialized dye wastewater on the environment and human health is photocatalysis [18]. The use of nanoparticles (NPs) or nanocomposites as a catalyst in photocatalytic dye degradation has attracted a lot of interest, and numerous studies have been published to support it [19].

Although noble metal-decorated systems (e.g., Ag/ZnO, Au/$TiO_2$) and transition metal oxide NPs like $TiO_2$ and ZnO have been thoroughly investigated for photocatalytic degradation of organic dyes, they frequently suffer from low visible-light activity and high recombination rates of photogenerated charge carriers. The pursuit for substitute photocatalysts has been spurred by these difficulties as well as the high price of noble metals [20]. Rare earth oxide NPs and materials doped with rare earth elements have recently become attractive options due to their better production of reactive species, reduced electron–hole recombination, and increased absorption of visible light. For example, rare earth dopants like $Er^{3+}$ in $TiO_2$ and Yb-based composites greatly enhance photocatalytic dye degradation when exposed to visible light, underscoring the increasing interest in rare earth systems for environmentally friendly wastewater treatment [21]. Because of their special electrical and structural characteristics, rare earth oxide NPs have become extremely attractive photocatalysts for the visible-light degradation of organic dyes. Compared to undoped metal oxides, rare earth elements can introduce localized electronic states and altered band gaps, thereby improving visible light absorption, enhancing photogenerated charge carrier separation, and reducing electron–hole recombination [22]. For example, a study by Lakshamanan K. et al. described the synthesis of silver NP/yttrium oxide with titanium carbide MXene (Ag/$Yb_2O_3$@$Ti_3C_2$) using coprecipitation and hydrothermal methods to produce a catalytic material for photocatalysis and a stable and high-performance electrode material for supercapacitors. Methylene Blue (MB) dye was used to test its photocatalytic efficiency. Additionally, the Ag/$Yb_2O_3$@$Ti_3C_2$ nanocomposite demonstrated exceptional photocatalytic activity, degrading MB dye by 97% in 75 min [23]. Another study described

a comparable green synthesis of $Y_2O_3$ NPs utilizing the sol–gel technique and aqueous leaf extracts of *Lantana camara L* (LC). The efficiency of these particles as a photocatalyst was investigated using LC $Y_2O_3$ NPs for the photocatalytic degradation of Rhodamine B. The findings showed that while the catalyst was present, 92% of the dye was broken down in 60 min, while when it was not, only 18% of the dye was broken down. This shows that the catalyst played a significant role in the dye's photocatalytic breakdown [24]. As a result, rare earth oxide NPs have shown potential in eradicating organic dyes and preventing water contamination from wastewater. In the current study, Orange II and Fast Green FCF dyes were used to investigate $Yb_2O_3$ NPs' dye degradation efficiency.

## 2. Materials and Methods

Analytical-grade reagents were used in the study as described in our previous manuscript [25].

## 3. Experimental

### *3.1. Synthesis of $Yb_2O_3$ NPs*

$Yb_2O_3$ NPs were fabricated through a co-precipitation method. 0.3 M aqueous NaOH solution was added dropwise to a 0.1 M $Yb(NO_3)_3{\cdot}5H_2O$ solution, as described in our previous manuscript [25]. The schematic representation of the synthesis process has been illustrated in Figure 1, as given in detail in our previously published paper [25].

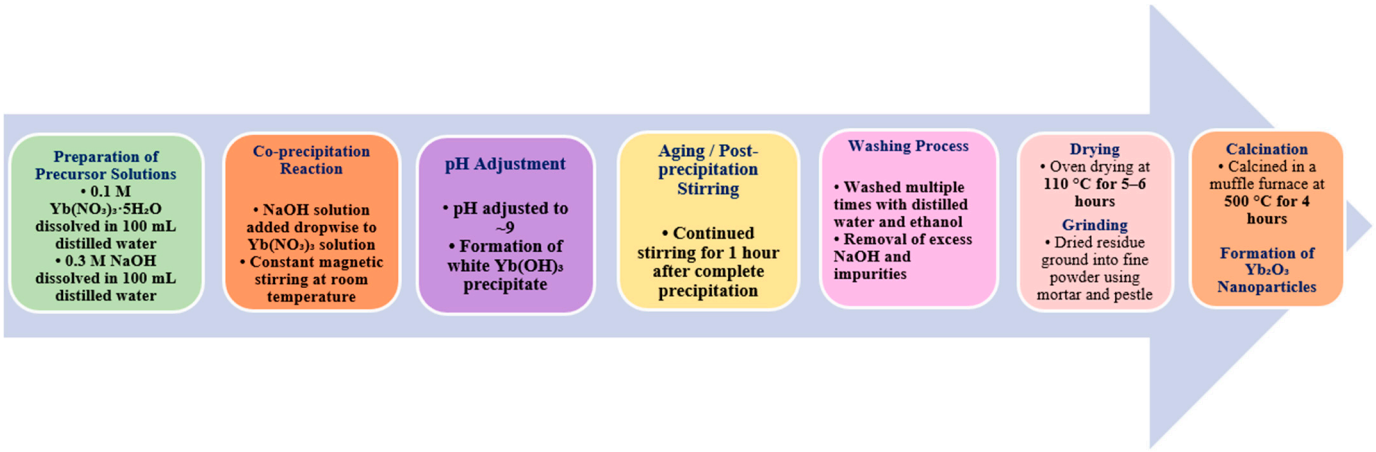


**Figure 1.** Schematic representation of synthesis of $Yb_2O_3$ NPs through co-precipitation method. Reproduced from Ref. [25] with permission from the Royal Society of Chemistry.

### *3.2. Photocatalytic Activity Evaluation*

The photocatalytic efficacy of the NPs was measured under visible light against Fast Green FCF and Orange II dyes using the reported methodology [25]. The reaction was carried out in a wooden dark box with a visible light source fitted in it. 50 mL of 10 ppm dye solution was taken and 25 mg of NPs were directly added to it and stirred in dark for 30 min. After that the solution was exposed to the visible light source with continuous stirring and 3 mL of sample was extracted every 15 min up till 105 min. After completion of the reaction, the catalyst was separated by centrifugation prior to UV–Vis analysis. The % degradation of the dye was estimated using Equation (1).

$$\%\text{Degradation} = (A_o - A_t)/A_o \quad (1)$$

where $A_t$ is the dye absorbance at time t, and Ao is the dye absorbance at the start. The dynamics of Orange II Sodium Salt and Fast Green FCF degradation were also investigated.

The degradation kinetics might be assessed by plotting ln ($C_t$) against time. The pseudo-first-order kinetic Equation (2) was used for the kinetic analysis.

$$\ln(C_o/C_t) = kt \quad (2)$$

Here, $C_o$ represents the initial concentration, $C_t$ denotes the concentration at time t, and k is the rate constant. The slope of the plot of $\ln(C_o/C_t)$ against time gives a rate constant, k.

## 4. Results and Discussion

### *4.1. Characterization*

The synthesized $Yb_2O_3$ NPs' UV-Vis absorption spectra (Figure 2a) show a notable absorption peak at 368 nm, which is caused by intrinsic electronic transitions from the valence to the conduction band. The broad band gap shown by this absorption pattern is typical of rare-earth metal oxides. According to the tauc plot, the band gap was 4.91 eV (Figure 2b) [25]. The FT-IR spectra (Figure 2c) were obtained in the 4000–400 $cm^{-1}$ range. The strong peaks at 578.54 $cm^{-1}$ and 416.55 $cm^{-1}$ confirmed Yb–O stretching vibrations, characteristic of metal–oxygen bonding in rare earth metal oxides [26,27]. According to our earlier publication, the XRD pattern matched with the JCPDS Card No. 43-1037 [25]. As described in our earlier paper, the SEM micrograph of $Yb_2O_3$ NPs revealed the irregularly shaped agglomerates made up of fine NPs. Smaller NPs have grouped to form larger clusters, giving the appearance of a heterogeneous particle distribution. The detailed characterization was given previously [25].

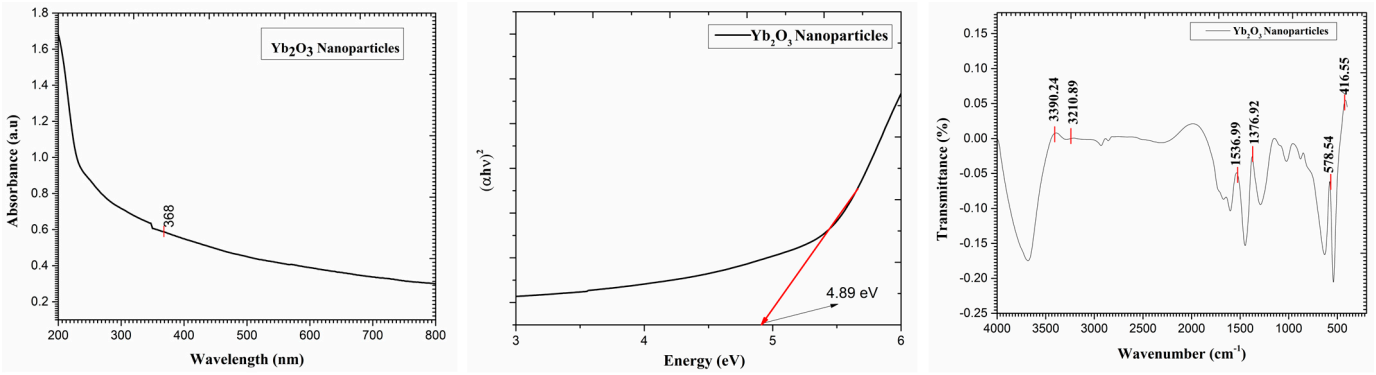


**Figure 2.** (**a**) UV-Vis spectra, (**b**) Tauc plot, and (**c**) FT-IR spectrum of $Yb_2O_3$ NPs [25].

### *4.2. Photocatalytic Potential*

Because of their extensive industrial use and their chemical stability, Fast Green FCF and Orange II are synthetic dyes that are widely acknowledged as persistent environmental contaminants. Because of its vivid color and water solubility, Fast Green FCF is a triarylmethane dye that is frequently applied as a colorant in food, cosmetics, pharmaceuticals, and textile products. However, when released in industrial effluents, its complex aromatic structure makes it resistant to biodegradation and contributes to its persistence in aquatic environments [28]. Orange II, sometimes referred to as Acid Orange 7, is a water-soluble anionic azo dye that is often employed in the paper, leather, and textile industries. Like other azo dyes, it has strong coloration and structural durability, making it challenging to remove using traditional wastewater treatment methods [29]. By decreasing light penetration, raising biochemical oxygen demand, and posing toxicological concerns to aquatic life and human health, these dyes can degrade water quality. This has prompted the development of sophisticated remediation techniques including photocatalytic degrada-

tion [30]. In our study, the photocatalytic dye degradation efficacy of $Yb_2O_3$ NPs was tested against Fast Green FCF and Orange II (Figure 3a,b) under visible light irradiation in 105 min. The dye degradation of Fast Green FCF with $Yb_2O_3$NPs was found to be 85.47% and follows pseudo-first-order kinetics with the rate constant of $1.6 \times 10^{-2}$ $min^{-1}$ ($R^2$ = 0.94045) as given in Figure 4a, while photodegradation of Orange II with $Yb_2O_3$NPs was found 83.09%, also following pseudo-first-order kinetics, and the rate constant was found to be $0.6 \times 10^{-2}$ $min^{-1}$ ($R^2$ = 0.96556) as given in Figure 4b. Figure 5 illustrates the % degradation versus time plot for both dyes.

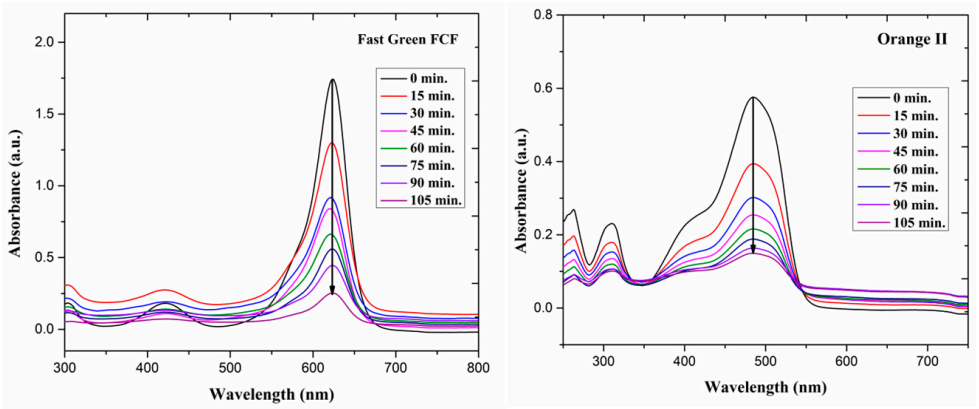


(**a**) (**b**)

**Figure 3.** Time-dependent UV-Vis spectra of (**a**) Fast green FCF and (**b**) Orange II treated with $Yb_2O_3$ NPs.

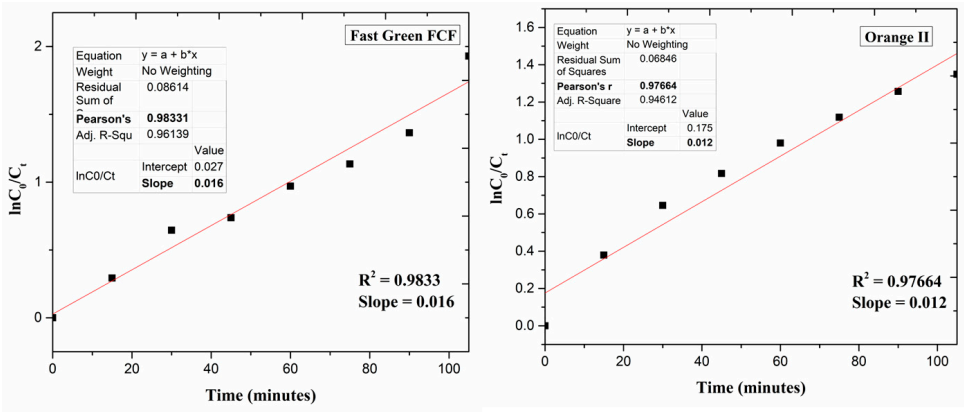


(**a**) (**b**)

**Figure 4.** Pseudo-first-order kinetic plots of ln(Co/Ct) vs. time for (**a**) Fast green FCF, and (**b**) Orange II treated with $Yb_2O_3$ NPs.

Due to its intrinsic semiconductor properties and electronic structure that are similar to well-known photocatalysts, $Yb_2O_3$, a lanthanide-based oxide semiconductor, has drawn research interest in photocatalytic applications. In particular, its wide band gap allows for the excitation of charge carriers under UV/visible irradiation, which is necessary for efficient photocatalysis. When exposed to the right light, $Yb_2O_3$'s band structure enables the production of photogenerated electrons and holes, making it a viable option for energy conversion research and environmental cleanup [27]. Furthermore, rare earth metal oxides generally have distinct 4f electronic configurations that can affect charge carrier dynamics and light absorption, which is known to improve charge separation and increase the range of photon absorption in metal oxides modified with lanthanide species. In comparison to undoped wide-band gap materials, the addition of rare earth oxides like $Yb_2O_3$ can improve photocatalytic performance by shifting optical absorption toward the visible range

and lowering electron–hole recombination rates. These features demonstrate the promise of $Yb_2O_3$ and related rare-earth oxides as light-active photocatalytic materials with adjustable optical and electrical characteristics that can be used to degrade pollutants when exposed to solar or visible light [31]. In photocatalytic reactions, electron holes are generated when the photocatalyst absorbs sufficient light energy [16].

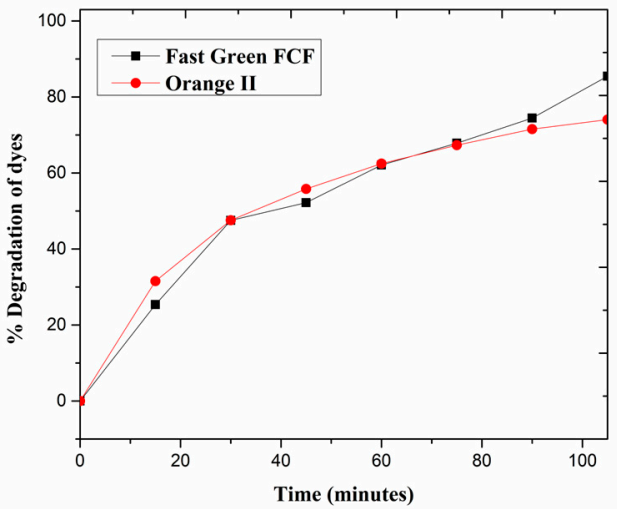


**Figure 5.** Degradation (%) of Fast green FCF and Orange II.

When photon energy is delivered to the surface of the NPs, the conduction band will excite electrons from the valence band, resulting in electron–hole pairs. Subsequently, the photogenerated electron holes convert hydroxide ions (OH) or water molecules ($H_2O$) into hydroxyl radicals (•OH). After the photoexcited electrons convert oxygen into superoxide radicals ($•O_2$), the H+ ions in water can then protonate these radicals to create hydroxyl radicals ($HO_2•$). These radicals fragment into the more reactive hydroxyl radical species OH• after being transformed into $H_2O_2$. The degradation of dyes depends on superoxide and hydroxyl radicals [32]. These reactive oxygen species attack the dye molecules adsorbed on the catalyst surface, leading to cleavage of the chromophoric groups responsible for color. Effective dye mineralization is achieved by further oxidizing the resultant intermediates, which yields inorganic ions, carbon dioxide, and water. The major inorganic ions formed during degradation include sulphate ($SO_4^{2-}$), nitrate ($NO_3^-$), and ammonium ($NH_4^+$). Basic qualitative chemical analysis verified the existence of these ions in the treated solution, supporting the mineralization of Orange II and Fast Green FCF dyes.

The reactions of the photocatalytic degradation pathway are listed below as Equations (3)–(10). The proposed mechanism of dye degradation has been illustrated in Figure 6.

$$\textbf{Activation:}\ \text{Catalyst} + h\nu \rightarrow e^- + h^+ \quad (3)$$

$$\textbf{ROS Generation:}\ h^+ + H_2O \rightarrow •OH + H \quad (4)$$

$$e^- + O_2 \rightarrow •O_2^- \quad (5)$$

$$•O_2^- + H^+ \rightarrow HO_2• \quad (6)$$

$$HO_2• + HO_2• \rightarrow H_2O_2 + O_2 \quad (7)$$

$$e^- + H_2O_2 \rightarrow •OH + OH^- \ (\text{or } H_2O_2 + h\nu \rightarrow 2•OH) \quad (8)$$

$$\textbf{Dye Degradation:}\ \text{Dye (colored)} + •OH/h^+/•O_2^- \rightarrow \text{Organic Intermediates (Decolorized)} \quad (9)$$

$$\textbf{Mineralization:}\ \text{Organic Intermediates} + •OH/h^+/•O_2- \rightarrow CO_2 + H_2O + SO_4^{2-} + NO^{3-} + NH^{4+} \quad (10)$$

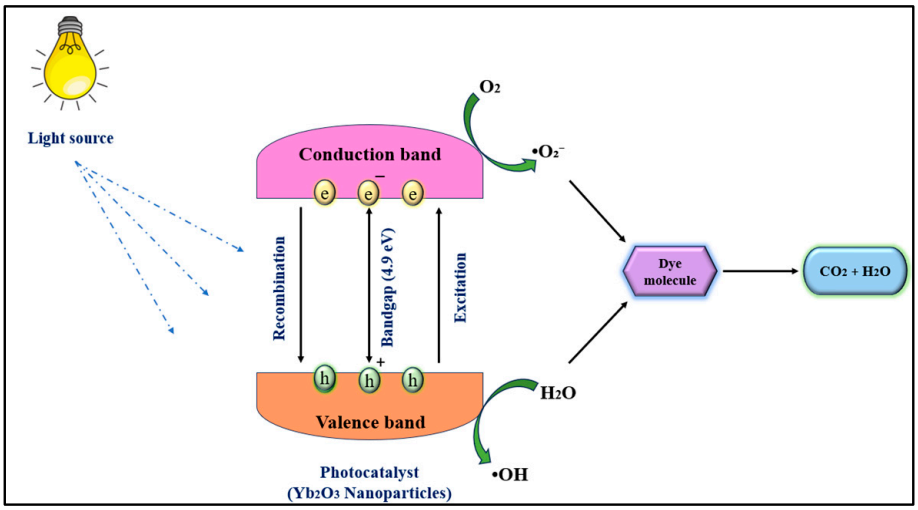


**Figure 6.** Probable mechanism of Fast Green FCF and Orange II dye degradation.

The photocatalytic potential of such NPs has also been shown in earlier studies. For instance, a recent work described the production of $CeO_2$ nanorods for the photocatalytic degradation of Congo Red (CR) dyes via hydrothermal synthesis and calcination. The results show that the CR solution degrades more quickly when exposed to UV light than when it is dark. Within 130 min, a high CR degradation efficiency of up to 97.7% was observed, demonstrating the rare-earth oxide's efficacy in photodegradation [33]. Similarly, another work described the synthesis of ZnO NPs doped with rare earth elements (Sm, Dy, and Nd) and evaluated their photocatalytic dye degradation effectiveness against Crystal Violet (CV) and Malachite Green (MG). The highest degrading efficiency for Dy-doped ZnO NPs was discovered to be 97.18% for MG and 98% for C [34]. Furthermore, some examples of rare earth NPs and rare earth doped nanomaterials effective in photocatalytic dye degradation are mentioned in Table 1.

**Table 1.** Some examples of rare earth NPs and rare earth-doped nanomaterials are effective in photocatalytic dye degradation.

| S.No. | Nanomaterial | Dye | Time (Minutes) | Source | Degradation % | Reference |
|---|---|---|---|---|---|---|
| 1 | $CeO_2$ NPs | MB | 80 | Sunlight | 75 | [35] |
| 2 | Sm-doped $CeO_2$ NPs | MB | 90 | UV Light | 80 | [36] |
| 3 | Eu-doped $CeO_2$ NPs | Rose Bengal | 120 | UV Light | 90 | [37] |
| 4 | La-doped ZnO | Rhodamine B | 40 | visible light | 82 | [38] |
| 5 | La-doped $TiO_2$ NPs | MB | 60 | visible light | 85 | [39] |
| 6 | Gd-doped ZnO NPs | MB | 120 | UV Light | 89 | [40] |
| 7 | Nd-doped ZnO NPs | MB | 180 | UV Light | 90 | [41] |
| 8 | Eu-doped $CeO_2$ NPs | Rhodamine B | 100 | UV Light | 70 | [42] |
| 9 | $La_2O_3$–$CeO_2$ | MB | 100 | UV Light | 80 | [43] |
| 10 | $La_2O_3$ NPs | MB | 100 | UV Light | 60 | [44] |

### *4.3. Recyclability of Nanoparticles*

The recyclability experiment for the NPs was performed for Fast Green FCF dye, up to third cycle to test the reusability of the photocatalyst. No significant loss in the degradation potential was observed, and after the third cycle, 83.11% degradation was observed as compared to 85.42%, of the fresh NPs (Figure 7). XRD analysis was also performed, after recovering the NPs via centrifugation from the treated dye solution to observe the changes in the crystalline structure of the NPs. The findings of the recyclability test show that the photocatalytic efficiency of the synthesized NPs does not significantly decrease even after

the third cycle. Furthermore, the XRD spectrum (Figure 8) of the recovered NPs, after the second cycle also does not show significant change, confirming that the crystalline structure of the NPs remains intact even after being employed as photocatalyst. The findings are consistent with the previous literature [45–47].

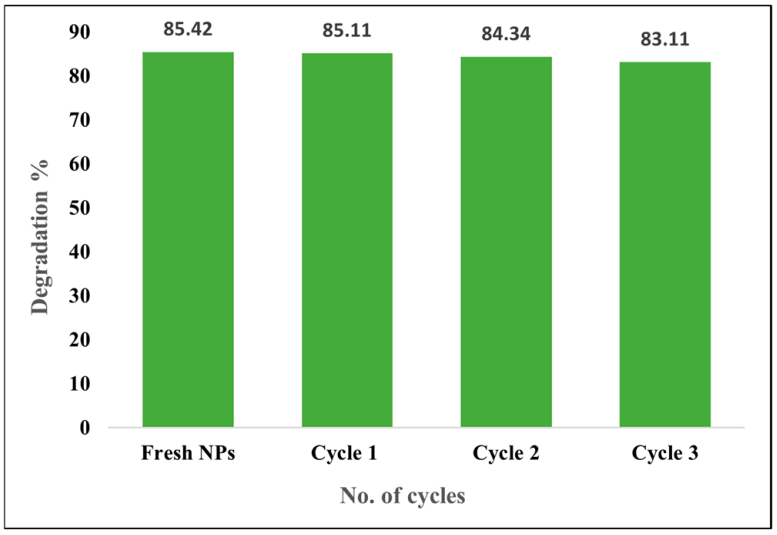


**Figure 7.** Graph showing the recyclability of the $Yb_2O_3$ NPs.

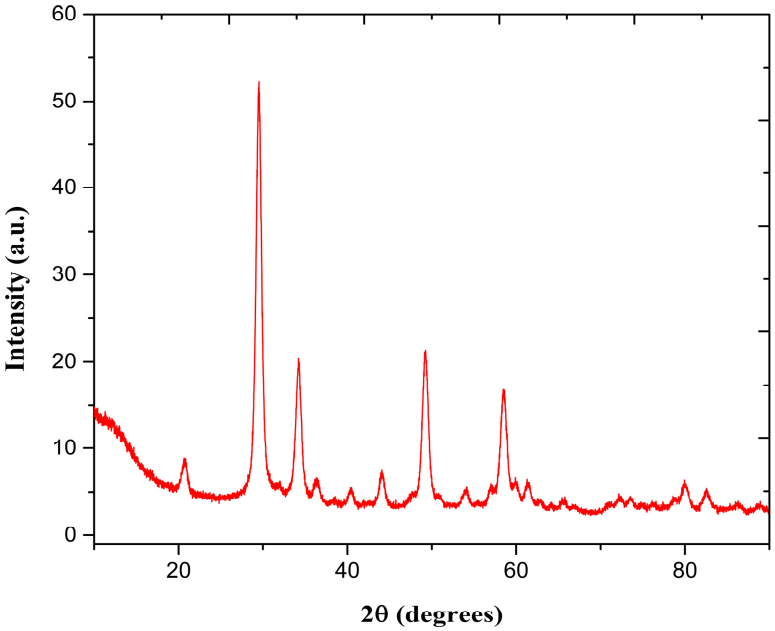


**Figure 8.** XRD spectra of $Yb_2O_3$NPs after III$^{rd}$ cycle.

## 5. Conclusions

Using a co-precipitation technique, $Yb_2O_3$ NPs were successfully produced and showed remarkable photocatalytic performance toward the degradation of Orange II and Fast Green FCF dyes in aqueous solutions. The catalyst's significant photocatalytic activity was demonstrated by its 105 min degradation efficiencies of 85.47% for Fast Green FCF and 83.09% for Orange II. These results demonstrate the outstanding ability of $Yb_2O_3$ NPs in eliminating dyes from wastewater, providing a practical and sustainable method for advanced water treatment applications in accordance with international environmental sustainability goals.

**Author Contributions:** Conceptualization, T.K.; proofreading, N.F.; writing—original draft preparation, writing—review and editing, E.V.; supervision, T.K. All authors have read and agreed to the published version of the manuscript.

**Funding:** This research received no external funding.

**Institutional Review Board Statement:** Not applicable.

**Informed Consent Statement:** Not applicable.

**Data Availability Statement:** The original contributions presented in this study are included in the article. Further inquiries can be directed to the corresponding author.

**Acknowledgments:** The authors acknowledge the support extended by the Department of Chemistry, Integral University, Lucknow and the R&D cell of the university for the Manuscript Communication Number (IU/R&D/2026-MCN0004230). The corresponding author acknowledges the support extended to her through the Outstanding Researcher Award for the year 2024 by the university.

**Conflicts of Interest:** The authors declare no conflicts of interest.

## References

1. Ahmed, Y.; Dutta, K.R.; Nepu, S.N.C.; Prima, M.; AlMohamadi, H.; Akhtar, P. Optimizing photocatalytic dye degradation: A machine learning and metaheuristic approach for predicting methylene blue in contaminated water. *Results Eng.* **2025**, *25*, 103538. [CrossRef]
2. Ahmed, Y.; Rahman, M.M.; Alam, M.S.; Miah, M.I.; Choudhury, M.S.H.; Alharbi, O.A.; Rahman, S.M. Harnessing neural network model with optimization for enhanced ciprofloxacin antibiotic adsorption from contaminated water: A transparent and objective framework. *J. Water Process Eng.* **2024**, *65*, 105724. [CrossRef]
3. Parida, S.; Mandal, A.K.; Behera, A.K.; Patra, S.; Nayak, R.; Behera, C.; Jena, M. A comprehensive review on phycoremediation of azo dye to combat industrial wastewater pollution. *J. Water Process Eng.* **2025**, *70*, 107088. [CrossRef]
4. Sharma, P.; Haq, N.; Ahmad, M.; Siddiqui, K.A. Mo@zinc-CP composite for dual applications: Luminescent detection of pesticides and photodegradation of organic dyes. *J. Mol. Struct.* **2025**, *1327*, 141249. [CrossRef]
5. Periyasamy, A.P. Textile dyes in wastewater and its impact on human and environment: Focus on bioremediation. *Water Air Soil Pollut.* **2025**, *236*, 562. [CrossRef]
6. Kumar, A.; Dixit, U.; Singh, K.; Gupta, S.P.; Beg, M.S.J. Structure and properties of dyes and pigments. In *Dyes and Pigments—Novel Applications and Waste Treatment*; IntechOpen: London, UK, 2021. [CrossRef]
7. Slama, H.; Chenari Bouket, A.; Pourhassan, Z.; Alenezi, F.; Silini, A.; Cherif-Silini, H.; Oszako, T.; Luptakova, L.; Golinska, P.; Lassaad, B. Diversity of synthetic dyes from textile industries, discharge impacts and treatment methods. *Appl. Sci.* **2021**, *11*, 6255. [CrossRef]
8. Yildirim, O.A.; Bahadir, M.; Pehlivan, E. Detrimental effects of commonly used textile dyes on the aquatic environment and human health: A review. *Fresenius Environ. Bull.* **2022**, *31*, 9329–9345.
9. Okoniewska, E. Sorption of selected dyes under dynamic conditions. *Desalin. Water Treat.* **2025**, *322*, 101172. [CrossRef]
10. Lopes de Sousa, M.; Bueno de Moraes, P.; Matos Lopes, P.R.; Nallin Montagnolli, R.; De Angelis, D.F.; Dino Bidoia, E. Contamination by Remazol red brilliant dye and its impact in aquatic photosynthetic microbiota. *Environ. Manag. Sustain. Dev.* **2012**, *1*, 129–138. [CrossRef]
11. Gita, S.; Hussan, A.; Choudhury, T.G. Impact of textile dyes waste on aquatic environments and its treatment. *Environ. Ecol.* **2017**, *35*, 2349–2353.
12. Islam, T.; Repon, R.; Islam, T.; Sarwar, Z.; Rahman, M.M. Impact of textile dyes on health and ecosystem: A review of structure, causes, and potential solutions. *Environ. Sci. Pollut. Res.* **2023**, *30*, 9207–9242. [CrossRef] [PubMed]
13. Chavan, R.B. Health and environmental hazards of synthetic dyes. *Garment Fash. Des.* **2013**, 6909.
14. Kumari, U. Textile dyes and their impact on the natural environment. In *Dye Pollution from Textile Industry: Challenges and Opportunities for Sustainable Development*; Springer Nature: Singapore, 2024; pp. 17–30. [CrossRef]
15. Saini, R.; Choudhary, K. Toxic potential of azo dyes: A broader understanding. In *Hazardous Chemicals*; Academic Press: London, UK, 2025; pp. 469–481. [CrossRef]
16. Fatima, N.; Veg, E.; Dwivedi, S.; Pandey, A.; Khan, T. Photocatalytic activity of $ZnFe_2O_4$ for the degradation of Fast Green FCF and Orange II. *Eng. Proc.* **2025**, *117*, 4. [CrossRef]
17. Ayub, A.; Wani, A.K.; Chopra, C.; Sharma, D.K.; Amin, O.; Wani, A.W.; Singh, A.; Manzoor, S.; Singh, R. Advancing dye degradation: Integrating microbial metabolism, photocatalysis, and nanotechnology for eco-friendly solutions. *Bacteria* **2025**, *4*, 15. [CrossRef]

18. Aina, A.R.N.; Patel, H.; Aich, S.; Roy, B.; Samanta, N.S.; Pal, B. Recent advances in ZnO-based photocatalysts for industrial dye degradation. *Discover Appl. Sci.* **2025**, *7*, 977. [CrossRef]
19. Lanjwani, M.F.; Tuzen, M.; Khuhawar, M.Y.; Saleh, T.A. Trends in photocatalytic degradation of organic dye pollutants using nanoparticles: A review. *Inorg. Chem. Commun.* **2024**, *159*, 111613. [CrossRef]
20. Kumar, K.H.; Ananda, H.T.; Ravishankar, D.K.; Madhu, H.; Thirumala, S. A review on nano metal oxides and their nanocomposites for photocatalytic degradation of dyes. *Sustain. Chem. One World* **2025**, *6*, 100055. [CrossRef]
21. El-Kholy, R.A.; Isawi, H.; Zaghlool, E.; Soliman, E.A.; Khalil, M.M.; Said, M.M.; El-Aassar, A.E.M. Preparation and characterization of rare earth element nanoparticles for enhanced photocatalytic degradation. *Environ. Sci. Pollut. Res.* **2023**, *30*, 69514–69532. [CrossRef]
22. Shukla, H.; Gautam, R.; Kumari, N. Photodegradation of dyes with rare-earth-doped metal oxide nanoparticles for wastewater treatment: A comprehensive review. *J. Phys. Chem. Solids* **2025**, *200*, 112593. [CrossRef]
23. Lakshmanan, K.; Dharman, R.K.; Kuppusamy, S.; Eswaramoorthy, N.; Viswanathan, M.R.; Ahmad, M.K.B.; Oh, T.H. Ag/$Yb_2O_3$@$Ti_3C_2$ nanocomposites as high-performance catalysts for energy storage and photocatalytic dye degradation. *Ceram. Int.* **2025**, *52*, 2264–2278. [CrossRef]
24. Govindasamy, R.; Govindarasu, M.; Alharthi, S.S.; Mani, P.; Bernaurdshaw, N.; Gomathi, T.; Ansari, M.A.; Alomary, M.N.; Atwah, B.; Malik, M.S.; et al. Sustainable green synthesis of yttrium oxide ($Y_2O_3$) nanoparticles using *Lantana camara* leaf extracts: Physicochemical characterization, photocatalytic degradation, antibacterial, and anticancer potency. *Nanomaterials* **2022**, *12*, 2393. [CrossRef]
25. Fatima, N.; Dwivedi, S.; Bansal, P.; Veg, E.; Mishra, V.; Khan, T. Environmental applications of ultrasonically synthesized and PEG-assisted $Yb_2O_3$/$ZnFe_2O_4$ nanocomposite for dye and herbicide degradation and electrochemical sensing of catechol. *Dalton Trans.* **2026**, *55*, 2200–2223. [CrossRef]
26. Kumar, S.; Chaudhary, G.R.; Chaudhary, S. Designing of surface-engineered ytterbium oxide nanoparticles as effective electrochemical sensing platform for dopamine. *J. Mol. Liq.* **2022**, *355*, 118929. [CrossRef]
27. Sarilmaz, A. Ytterbium oxide nanofibers: Fabrication and characterization for energy applications. *Turk. J. Chem.* **2022**, *46*, 1694–1701. [CrossRef] [PubMed]
28. Sudhakaran, G.; Priya, P.S.; Murugan, R.; Haridevamuthu, B.; Kannan, J.; Almutairi, S.M.; Arockiaraj, J. Follicular and neural toxic effect of prolonged exposure of synthetic dye Fast Green FCF (E143): Insights from zebrafish model. *Toxicol. Lett.* **2025**, *413*, 111726. [CrossRef]
29. van Bommel, R.; de Keijzer, M. The early azo dyes: Aniline yellow, Bismarck brown, chrysoidine, orangés, fast red A. In *Bright Colours from the Past: The History, Chemistry, Characterisation and Application of Synthetic Dyes Between 1856 and 1914*; Springer Nature: Cham, Switzerland, 2025; pp. 223–246. [CrossRef]
30. Al-Tohamy, R.; Ali, S.S.; Li, F.; Okasha, K.M.; Mahmoud, Y.A.G.; Elsamahy, T.; Sun, J. A critical review on the treatment of dye-containing wastewater: Ecotoxicological and health concerns of textile dyes and possible remediation approaches for environmental safety. *Ecotoxicol. Environ. Saf.* **2022**, *231*, 113160. [CrossRef]
31. Mehtab, A.; Ahmed, J.; Alshehri, S.M.; Mao, Y.; Ahmad, T. Rare earth doped metal oxide nanoparticles for photocatalysis: A perspective. *Nanotechnology* **2022**, *33*, 145706. [CrossRef]
32. Saridewi, N.; Utami, D.J.; Zulys, A.; Nurbayti, S.; Putri, A.R.; Kamal, R. Utilization of *Sansevieria trifasciata* extract for green synthesis of $ZnFe_2O_4$ nanoparticles as visible-light-responsive photocatalyst for dye degradation. *Case Stud. Chem. Environ. Eng.* **2024**, *9*, 100745. [CrossRef]
33. Rianjanu, A.; Mustamin, A.S.P.; Melati, E.K.A.; Aflaha, R.; Khamidy, N.I.; Utami, M.; Taher, T. Photocatalytic degradation of aqueous Congo red dye pollutants by rare-earth metal oxide ($CeO_2$) nanorods. *Colloids Surf. A Physicochem. Eng. Asp.* **2024**, *682*, 132919. [CrossRef]
34. Dhiman, P.; Rana, G.; Kumar, A.; Dawi, E.A.; Sharma, G. Rare earth doped ZnO nanoparticles as spintronics and photocatalysts for degradation of pollutants. *Molecules* **2023**, *28*, 2838. [CrossRef] [PubMed]
35. Farooq, U.; Zahra, S.T.; Ibrahim, M.; Naseem, K.; Khan, M.E.; Ali, W.; Zakri, W. Green-synthesized $CeO_2$ nanoparticles for photo-induced degradation of methylene blue and $CO_2$ photoreduction: Optimization by RSM-CCD model. *J. Taiwan Inst. Chem. Eng.* **2025**, *174*, 106220. [CrossRef]
36. Joseph, A.; Ayyappan, A.; Subair, T.; Pandibayal, M.; Nair, S.; Ramany, R.; Thomas, S. Pure and Sm-doped $CeO_2$ nanoparticles: Insights into room-temperature ferromagnetism and photocatalytic dye degradation. *ChemistrySelect* **2023**, *8*, e202301020. [CrossRef]
37. Madaan, V.; Bhankar, V.; Singh, P.; Mohan, B.; Kumar, K. Oxygen vacancy generation in ceria via Eu(III) doping for accelerated charge separation and UV-driven photodegradation of Rose Bengal dye. *Opt. Mater.* **2025**, *166*, 117213. [CrossRef]
38. Zhou, Z.; Yang, W.; Zhong, J.; Peng, H.; Zhao, S. La-doped ZnO/SBA-15 for rapid and recyclable photodegradation of rhodamine B under visible light. *Molecules* **2025**, *30*, 4800. [CrossRef]
39. Bayan, E.; Volkova, M.; Tolstunov, M.; Chernyshev, A. Synthesis of La-doped $TiO_2$ nanoparticles with enhanced photocatalytic activity. *Nanotechnol. Environ. Eng.* **2025**, *10*, 17. [CrossRef]

40. Alasmari, A.; Alresheedi, N.M.; Alzahrani, M.A.; Aldosari, F.M.; Ghasemi, M.; Ismail, A.; Aboraia, A.M. High-performance photocatalytic degradation by Gd-codoped ZnO nanocomposites: A systematic study. *Catalysts* **2024**, *14*, 946. [CrossRef]
41. Alam, U.; Khan, A.; Ali, D.; Bahnemann, D.; Muneer, M. Comparative photocatalytic activity of sol–gel-derived rare earth metal (La, Nd, Sm and Dy)-doped ZnO photocatalysts for dye degradation. *RSC Adv.* **2018**, *8*, 17582–17594. [CrossRef]
42. Toloman, D.; Popa, A.; Sonher, R.B.; Bortnic, R.; Marinca, T.F.; Perhaita, I.; Filip, M.; Mesaros, A. Enhancing the photocatalytic activity and luminescent properties of rare-earth-doped $CeO_2$ nanoparticles. *Appl. Sci.* **2024**, *14*, 522. [CrossRef]
43. Rahman, A.; Kumar, M. Improved photocatalytic activity for removal of methylene blue dye from aqueous solutions with $La_2O_3$-modified ceria heterostructured binary oxide nanocomposite particles. *J. Polym. Compos.* **2025**, *13*, 514–532.
44. Kaviyarasu, K.; Matinise, N.; Mayedwa, N.; Mamba, B.B.; Dlamini, T.S. Time-dependent hydrothermal synthesis of $La_2O_3$ nanoparticles for the photocatalytic degradation of methylene blue dye. *J. Mater. Chem. C* **2024**, *12*, 89–98. [CrossRef]
45. Veg, E.; Raza, A.; Bansal, P.; Rai, S.; Sharma, S.; Dwivedi, S.; Fatima, N.; Gupta, R.; Joshi, S.; Khan, A.R.; et al. Ultrasonically Synthesized CuO–Thiosemicarbazone Nanoconjugates: A Study on Interfacial Interactions and Synergistic Biological and Photocatalytic Effects. *Surf. Interfaces* **2025**, *72*, 107271. [CrossRef]
46. Veg, E.; Raza, A.; Bansal, P.; Rai, S.; Sharma, S.; Gupta, R.; Dwivedi, S.; Joshi, S.; Khan, A.R.; Khan, T. Synthesis, and characterization of ZnO–thiosemicarbazone nanoconjugates for enhanced biological and photocatalytic activity through surface synergy. *Inorg. Chem. Commun.* **2025**, *181*, 115265. [CrossRef]
47. Jabeen, S.; Siddiqui, V.U.; Sharma, S.; Rai, S.; Bansal, P.; Bala, S.; Raza, A.; Ahmad, M.I.; Khan, A.R.; Khan, T. A novel green synthesis of $CuFe_2O_4$ Nanoparticles from Cissus rotundifolia for photocatalytic and antimicrobial activity evaluation. *J. Alloys Compd.* **2024**, *984*, 174020. [CrossRef]